Forensic Facial Reconstruction using Mesh Template Deformation with Detail Transfer over HRBF

Rafael Romeiro, Ricardo Marroquim, Claudio Esperança
Computer Graphics Lab
COPPE/UFRJ
Email: {romeiro, marroquim, esperanc}@cos.ufrj.br

Andreia Breda, Carlos Marcelo Figueredo
School of Dentistry, Department of Periodontology
UERJ
Email: andreiacrisbreda@gmail.com

Fig. 1. Input skull

Fig. 2. Output facial reconstruction achieved by our method

***Abstract*—Forensic facial reconstruction is the application of anthropology, art and forensic science to recreate the face of an individual from his skull. It is usually done manually by a sculptor with clay and is considered a subjective technique as it relies upon an artistic interpretation of the skull features. In this work, we propose a computerized method based on anatomical rules that systematically generates the surface of the face through a HRBF deformation procedure over a mesh template. Our main contributions are a broader set of anatomical rules being applied over the soft tissue structures and a new deformation method that dissociates the details from the overall shape of the model.**

***Keywords*-facial reconstruction; hrbf; detail transfer; human identification; forensic anthropology; forensic science;**

I. Introduction

In forensic science, human skeletal remains may be identified with methods of high accuracy like DNA analysis or comparison with antemortem dental records. Sometimes, these traditional means of identification may not be possible or practical due to several reasons (lack of antemortem information, edentulousness, condition of the remains, cost etc). In these cases, facial reconstruction can be used as a last resort for positive identification or to narrow the search field.

In traditional facial reconstruction the first step is the addition of markers to indicate the depth of the tissue at specific points (craniometric points) over a skull or skull replica. The tissue depth data is usually obtained from a lookup table defined from previous studies and based on ancestry, gender and age. The muscles are then modeled with clay following anatomical guidelines regarding their origins and insertions. Finally, the skull is filled with clay until all the depth markers have been covered. In this process, the face morphology is determined by the artist employing different standards related to the facial features [1]. Methodologies using digital models usually rely on the same manual process using 3D modeling tools.

The traditional methodologies (manual or digital) are very time consuming and are prone to artistic subjectivity, whereas an automatic computer methodology can be performed in just a few minutes with reproducible deterministic results. The main challenge regarding automatic methodologies is the adaptation of the traditional guidelines to be applied in an automatic manner inside a geometrically accurate environment.

Our goal in this work is to produce automatic facial reconstructions with all the soft tissue structures without being

1530-1834/14 $31.00 © 2014 IEEE
DOI 10.1109/SIBGRAPI.2014.25

biased toward predefined templates.

Contributions: The contributions of this work are twofold. First, we adapt a broad set of anatomical rules, giving them strict geometric interpretation so that they can be computed and simultaneously applied. Second, we propose a template deformation method that takes into account all the anatomical rules over the soft tissue structures while suiting them to the overall shape of the skull.

In addition, by allowing a combination of different methodologies, this work also contributes as a validation tool for the techniques from the facial reconstruction literature, since it is deterministic and thus free from human interpretation.

A. Related work

Computerized automation of the facial reconstruction has been previously proposed in other works. Most of these related works use craniometric points as a base for facial reconstruction, however they employ different interpolation and restriction techniques.

Pascual et al. [2] propose a method to interpolate the position of the outer ends of virtual tissue depth markers analogous to those used in the manual method. The result of this method is a triangular mesh without soft tissue structures like eyes, nose, ears and mouth. The lack of those structures imposes an enormous difficulty on identification.

Vanezis et al. [3] propose the use of a database of facial templates from which a set of templates are selected according to the skull anthropological criteria (age, gender and ethnicity). The soft tissue points corresponding to the craniometric points are marked on the templates. The selected templates are then deformed so that their soft tissue points match the corresponding estimated points from the skull given the tissue depth data. In this way, the templates are adapted to accommodate the skull. Nevertheless, the soft tissue structures are not significantly modified biasing the results toward the database's templates.

Kahler et al. [4] also propose the deformation of a template given the craniometric points restrictions. However, they perform a second deformation with additional reconstruction hints by inserting anatomical rules regarding the nose and mouth. They also create a virtual muscle layer that allows animations of facial expressions. However, the muscles are added after the face reconstruction, and thus are not used as restrictions to model the face.

Hu et al. [5] propose a hierarchical dense deformation of a global model and three local models (eyes, nose and mouth) with a two-step fusion procedure to integrate the local and global results smoothly. This related work is not based on predefined craniometric points and thicknesses. Instead, it uses a pair of template skull and template face with a dense registration method to build a point-to-point correspondence between them. The reconstruction is done by an iterative method that adjusts the template skull to gradually approach the input skull, using the point-to-point correspondence to produce the face at the end.

Turner et al. [6] describe another method that is not based on craniometric points and thicknesses. It relies on a CT scans database of skulls and corresponding faces. For a new questioned input skull, between 50 and 150 known skulls from the database are deformed with a warping process to approximate it. Then, the corresponding faces of the deformed skulls are also deformed with the same warping process, resulting in a set of possible faces for that skull shape. Through a principal components analysis of all the deformed faces, it is possible to find an average face as well as a set of eigenvectors that spans the "face-space". These eigenvectors are variation vectors that have statistical significance and can be applied with different weights over the average face to reconstruct faces with a statistically quantifiable likelihood of occurring in the general population.

Duan et al. [7] proposes a partial least squares regression (PLSR) based mapping from skull to skin in the tensor spaces taking into account the age and body mass index (BMI) attributes. The regression model is trained from a database of 200 whole head CT scans on voluntary persons from China. Using the regression model, a new skin surface can be reconstructed from an input skull, an age and a BMI.

B. Technique overview

Our method begins with the manual identification of the craniometric points on the skull. Then, the predefined thickness of soft tissue for each craniometric point is used in conjunction with the normals obtained from the skull model to produce an initial set of target face points. This set is increased with more points as each anatomical rule is applied. When all the desired anatomical rules have been used, the final set of target face points is achieved. For each point in the set of target face points, there is a corresponding origin point in the template face model. A HRBF surface is created from the set of target face points and another from the set of origin template points. The differences between the template and the HRBF surface created from the set of origin template points are then added to the HRBF surface created from the set of target face points, thus yielding the final result of the facial reconstruction.

II. Craniometric points restriction

To the best of our knowledge, there is no automated method to identify the craniometric points. In fact, these points many times have no geometrical hints, and are based solely on the specialist's experience and notion of anatomy. Therefore, an expert is required to manually mark them on the virtual skull. An application was developed to display and manipulate the skull, allowing the expert to place markers over it's surface. The thickness (soft tissue depth) are manually inserted, but they could also be automatically recovered from a given table using some sort of identification for the points.

For each marked point on the skull's mesh, a smoothed normal vector is computed by averaging the normals of neighboring vertices. Combining the normal vector with the thickness of each point, a new point is defined, estimated to

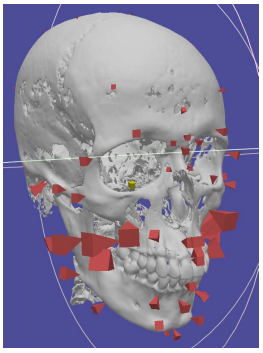

(a) Craniometric points with thickness applied in the normal direction

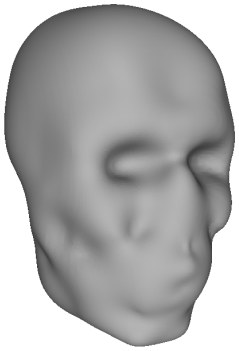

(b) Surface generated with HRBF from displaced craniometric points and normals

Fig. 3. Craniometric points restriction

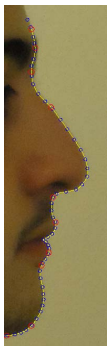

(a) Curve acquisition

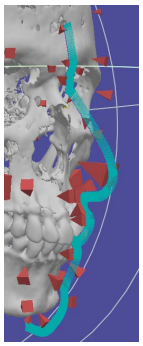

(b) Curve adaptation

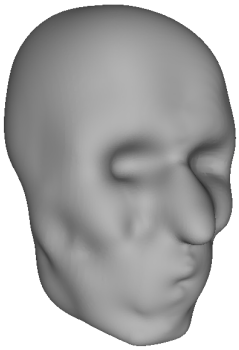

(c) Reconstruction with additional profile curve restriction

Fig. 5. Curves restriction

lie on the face's soft tissue (Fig. 3a). This process defines the input of our method, that is, a set of points on the face corresponding to the craniometric points.

From the position of those points and their normals on the skull, an implicit surface could be readily generated using HRBF [8] for example. Points can then be sampled from this surface for visualization or mesh reconstruction. Nonetheless, without the addition of anatomical rules, the result is a very crude face without nose, ears, eyes or mouth (Fig. 3b), unsuitable for recognition purposes. In order to add details, the prior knowledge of how a human face looks like must be defined apart from the input skull.

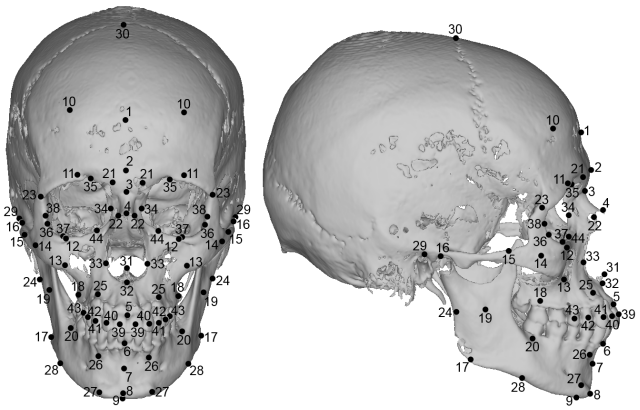

Fig. 4. Craniometric point (Table I) positions in frontal view and side view

III. Curves restriction

A first attempt to add these missing structures was through two-dimensional curves. The curves were obtained manually from a profile image of a face, and defined as a Catmull-Rom spline [9]. The points corresponding to the craniometric points on soft tissue were marked on the image (Fig. 5a). By matching the marked points of the curve with those already calculated from the skull, the best position and orientation of the curve in relation to the skull is retrieved. The curve is then deformed as rigidly as possible using a moving least squares approach [10] for an exact fit (Fig. 5b).

Sample points of the adapted curve are taken and their normals evaluated. The adapted curve points are then fed to the HRBF surface generation together with the other points from the soft tissue (Fig. 5c). Even though it is a clear improvement from the bare HRBF reconstruction, apart from the profile curve, it is hard to define other curves over the face that are easily traceable and identified over the skull. Even more, the adapted curve seems to not provide sufficient details necessary for identification.

IV. Anatomical restrictions

To improve the quality of the result, even more anatomical knowledge must be fed to the system. However, one must be extremely cautious not to bias the result towards the features of the extra input information. In order to lessen this issue, a series of anatomical rules were surveyed from the facial reconstruction literature in order to add new restrictions computed from the input skull itself.

Most anatomical rules make reference to some anatomical planes. The most important planes are the Frankfurt plane, which separates the head into superior and inferior parts, the Midsagittal plane, which separates the head into left and right parts, and the Coronal plane, which separates the head into anterior and posterior parts. It is important to note that these three planes are orthogonal to each other. In order to use them on the following rules, they must be defined relative to the skull. This is accomplished by defining the Frankfurt plane as the plane containing the left suborbital point, the left porion point and the right porion point. The Midsagittal plane is then defined as the plane orthogonal to the Frankfurt plane containing the prostion point and the bregma point. Finally, the Coronal plane is defined as the plane orthogonal to the Frankfurt plane and orthogonal to the Midsagittal plane containing the left porion point. (Fig. 6)

TABLE I
SUMMARY OF THE CRANIOMETRIC POINTS USED

	Point name	Use	Skin Thickness (mm) * non-Brazilian values
1	Supraglabella	Skin thickness	5.27
2	Glabella	Skin thickness	6.07
3	Nasion	Skin thickness, Nasal profile (Rynn et al., Prokopec et al.)	7.37
4	Rhinion	Skin thickness, Nasal tip curve, Nasal profile (Rynn et al., Prokopec et al., Two tangent)	3.27
5	Prostion / Supradentale	Skin thickness, Midsagittal plane, Nasal profile (Prokopec et al.)	9.72
6	Infradentale	Skin thickness	9.36
7	Chin-lip fold / Supramentale	Skin thickness	10.64
8	Gnation / Mental eminence	Skin thickness, Lip fissure level	10.13
9	Subgnation / Menton	Skin thickness	7.38
10	Frontal eminence (bilateral)	Skin thickness	5.00
11	Supraorbital (bilateral)	Skin thickness	8.12
12	Suborbital (bilateral)	Skin thickness, Frankfurt plane	6.35
13	Inferior malar (bilateral)	Skin thickness	20.68
14	Lateral orbit (bilateral)	Skin thickness	9.57
15	Zygomatic arch (bilateral)	Skin thickness	9.45
16	Supraglenoid (bilateral)	Skin thickness	13.23
17	Gonion (bilateral)	Skin thickness	14.42
18	Supra M2 (bilateral)	Skin thickness	24.83
19	Occlusal line (bilateral)	Skin thickness	22.28
20	Sub M2 (bilateral)	Skin thickness	23.26
21	Lateral glabella (bilateral)	Skin thickness	5.9 *
22	Lateral nasal (bilateral)	Skin thickness, Nasal tip curve	4.8 *
23	Mid lateral orbit (bilateral)	Skin thickness	4.7 *
24	Mid masseter (bilateral)	Skin thickness	16.7 *
25	Supra canina (bilateral)	Skin thickness	10.2 *
26	Sub canina (bilateral)	Skin thickness	9.3 *
27	Mental tubercule anterior (bilateral)	Skin thickness	9.2 *
28	Mid mandibular (bilateral)	Skin thickness	9.5 *
29	Porion (bilateral)	Frankfurt plane, Coronal plane	N/A
30	Bregma	Midsagittal plane	N/A
31	Acanthion / Nasospinale	Nasal profile (Rynn et al., Two tangent)	N/A
32	Subnasal / Subspinale	Nasal profile (Rynn et al.), Lip fissure level	N/A
33	Lateral piriform margin (bilateral)	Nasal width (Hoffman et al., 5/3 rule)	N/A
34	Medial orbital margin (bilateral)	Eyeball position, Palpebral fissure width	N/A
35	Supra orbital margin (bilateral)	Eyeball position, Palpebral fissure width	N/A
36	Lateral orbital margin (bilateral)	Eyeball position, Palpebral fissure width	N/A
37	Infra orbital margin (bilateral)	Eyeball position, Palpebral fissure width	N/A
38	Posterior lateral orbital margin (bilateral)	Eyeball position, Palpebral fissure width	N/A
39	Superior central incisor (bilateral)	Dental arch curvature, Philtrum width	N/A
40	Superior lateral incisor (bilateral)	Dental arch curvature	N/A
41	Superior canine (bilateral)	Dental arch curvature, Mouth width (Stephan et al.)	N/A
42	Superior first premolar (bilateral)	Dental arch curvature	N/A
43	Superior second premolar (bilateral)	Dental arch curvature, Mouth width (Lebedinskaya et al.)	N/A
44	Infraorbital foramen (bilateral)	Mouth width (Stephan et al.)	N/A

A. Nose

With the regressions presented by Rynn et al. [11], the nasal length, nasal height and nasal depth can be computed from the nasion-acanthion, rhinion-subspinale and the nasion-subspinale distances yielding the nose tip point and the subnasal point positions. Alternatively, the two tangent method [12] can be used to adjust the nasal tip, which showed better results in some cases. Yet a third approach may be used to define the entire nasal profile from the shape of the piriform aperture [13].

In conjunction with these three methods, the nasal width can be calculated from the lateral margin of the piriform aperture with either the addition prediction formulas or multiplication prediction formulas as described by Hoffman et al. [14] or the 5/3 rule [15].

Davy-Jow et al. [16] states that the nose tip curvature mimics the curvature of the superior portion of the nasal aperture when the head is tilted upward so that the pronasale point is superimposed over the rhinion point. We implemented a generalization of this rule by obliging the nose tip curvature to be a scaled version of the curvature of the superior portion of the nasal aperture for any specific tilt angle (which is reduced to the previous case with a scale value of one for the pronasale-rhinion superimposition). Within the scope of the generalized rule, the best results were obtained when the rhinion point was superimposed over the nasion point.

B. Eyes

The eyeball positions as well as the canthi positions were calculated from the margins of the orbital cavity keeping

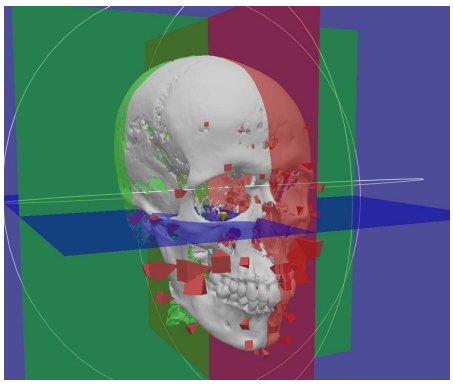

Fig. 6. Anatomical planes: Frankfurt plane (blue), Midsagittal plane (red) and Coronal plane (green)

the proportions of the average values given by Stephan et al. [17] [18].

The average value of the height of the palpebral fissure is 10.2mm [19], the inferior palpebral margin should touch the iris while the superior palpebral margin should cover 2mm of the iris [20]. These three restrictions can be easily met at the same time by placing the superior palpebral margin 4.1mm over the pupil and the inferior palpebral margin 6.1mm under the pupil, thus setting the iris diameter to 12.2mm, which is in the high end of its range [21].

C. Mouth

For the mouth, the lip fissure was placed at a distance of the subnasal point equal to 31,2% of the distance between the subnasal and gnation points [22].

The mouth width can be obtained from formulas based on the length of the arc between the two premolars [23], on the length of the arc between the two superior canines [24] or on the distance between the two infraorbital foramen [18]. This width can be imposed as an euclidean distance or over an arc.

The upper and lower lip thickness can be predicted from the height of the upper and lower incisors [25]. The cupid's bow shape can be defined from the average central bow angle [26] coupled with the width of the philtrum, which can be estimated from the distance between the central incisors [27].

D. Ears

No methodological proposal was found to reconstruct the ear from the skull. Therefore, average measures for the width and length of the ear as well as the width and height of the ear lobe were used [28].

E. Reconstruction configuration

To select which combination of anatomical rules will be applied, a configuration screen was created inside our application. It is also in this screen that the gender and ethnicity are set. The Table II displays a summary of the options.

TABLE II
SUMMARY OF THE RECONSTRUCTION OPTIONS

Template	Gender	• Male • Female
	Ethnicity	• Caucasoid • Negroid • Mongoloid
Nose	Nasal Width	• 5/3 rule [15] • APF [14] • MPF [14]
	Nasal Profile	• Linear regression [11] • Two tangents [12] • Profile points [13]
	Nasal Tip Curve	• Nasal aperture curvature [16] • Generalized
Eyes	Eyeball Position	• Ocular orbit proportions [18]
	Palpebral Fissure Width	• Ocular orbit proportions [17]
	Palpebral Fissure Height	• Average [19] [20]
Mouth	Lip Fissure Level	• 31.2% subnasal-gnation [22]
	Mouth Width	• Premolar distance [23] • Intercanine distance [24] • Foramen distance [18]
	Lip Thickness	• Incisor heights [25]
	Cupid's Bow Angle	• Average [26]
	Philtrum Width	• Incisors distance [27]
Ears	Ear Length	• Average [28]
	Ear Width	• Average [28]
	Ear Lobe Width	• Average [28]
	Ear Lobe Height	• Average [28]

V. TEMPLATE RESTRICTIONS

Even with the addition of the extra points from the anatomical restrictions, there isn't enough sampling information for a proper facial reconstruction. One alternative is to use a template mesh for each soft tissue structure (nose, ear etc...), which is placed, oriented and deformed to match the restrictions outlined above. Points and normals from the meshes are then sampled and fed to the HRBF algorithm (Fig. 7). By adding only the necessary pieces of templates we minimize the bias towards the input structures. The downside is that by separately placing these meshes, the way that the soft tissues structures are connected to each other are not entirely respected (the eye balls with the eye lids, the eye lids with the nose, the nose with the mouth and so on). The way they are linked is important and it is difficult to geometrically specify where one structure ends and another begins.

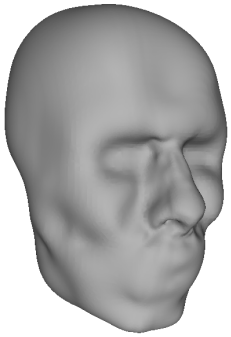

Fig. 7. Reconstruction with nose mesh restriction

Therefore, instead of separate meshes, a full template model is employed (Fig. 10a, Fig. 11a, Fig. 12a). On one hand, by limiting the result to be a deformation of this template model, we can ensure that the result will resemble a human face. On the other hand, the risk of getting biased results is much greater. Hence, all the previous anatomical restrictions are applied and a detail transfer approach is used to guarantee that the template model will suffer enough modifications to achieved an as unbiased as possible result.

As a matter of fact, with the complete model for the face there are no gaps on the surface to be covered and the HRBF algorithm can be replaced by a simpler MLS deformation [10]. One needs only to assign the soft tissue points on the template corresponding to the craniometric points and the extra anatomical restrictions. Nonetheless, the use of MLS proved inappropriate as the deformations end up being very local, eventually introducing points of high frequency (sharp edges) and still being significantly biased towards the overall shape of the template (Fig. 10b, Fig. 11b, Fig. 12b).

To restore the smoothness necessary to represent a human face and avoiding biased results, a detail transfer based on the HRBF deformation is proposed. Two implicit surfaces are produced: one from the points calculated from the input skull to be the target (Fig. 8b) and one from the corresponding points picked on the template model to be the origin (Fig. 8a). These surfaces can be seen as basic low-frequency structures of the faces, i.e., lacking details. The details from the template model are stored as difference vectors from the points on the template mesh to the HRBF surface. These detail vectors are then transferred to the skull's HRBF surface to restore the facial restrictions (Fig. 9). This detail transfer procedure automatically adapts the soft tissue structures to the overall shape of the input skull and preserves the template mesh topology.

To produce an HRBF surface, as opposed to an RBF surface, a normal vector must be provided for each interpolation point. To produce the origin HRBF surface, the normals of the template mesh are used, since it is a simplification of this mesh. For the target HRBF surface, ideally the subject skin normals would be used. However, this information is not available for the reconstruction. The normals of the template mesh are skin normals, but not of the subject, while the normals of the input skull are particular to the subject, but the skull normal may not be related to the skin normal depending on the region. Bearing this in mind, the skull normal was used where the skin thickness was small enough so that the skin normal was related to the skull normal (skin thickness smaller than 5 mm), otherwise, the template normal was used.

Note that the detail transfer procedure alone is not enough to achieve plausible results. Fig. 14 shows a reconstruction with the anatomical restrictions left aside. In this case the deformation is unable to adapt the specificities of the soft tissue structures to the skull.

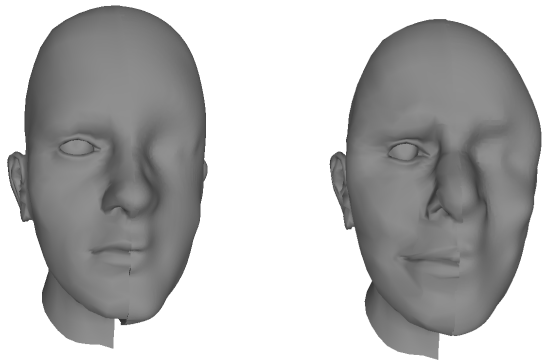

(a) Template (left half) and origin HRBF from template (right half)

(b) Detail transfer result (left half) and target HRBF from skull (right half)

Fig. 8. HRBF face approximation for detail transfer

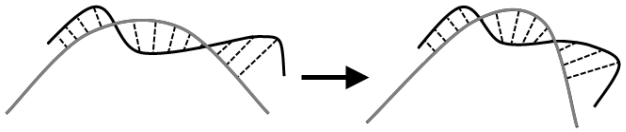

Fig. 9. The detail (black) over the smooth HRBF surface (grey) being transferred to the other smooth HRBF surface

VI. Results

Our test subjects underwent CT scans and had their faces scanned to produce input skulls models and corresponding ground truths. With the help of a professional in the field of forensic medicine, a set of 57 craniometric points were marked for each skull. The thicknesses entered were average measures for Brazilians [29] and a few non-Brazilian measures [30]. The exact thickness values used are displayed at the Table I.

The method described in this work produced very accurate results as one may evaluate from the real scanned face (Fig. 10d, Fig. 11d, Fig. 12d) of the test subjects. However, the use of a template suitable for the gender, age and ethnicity is still required. An example of bad template usage can be seen in Fig. 13.

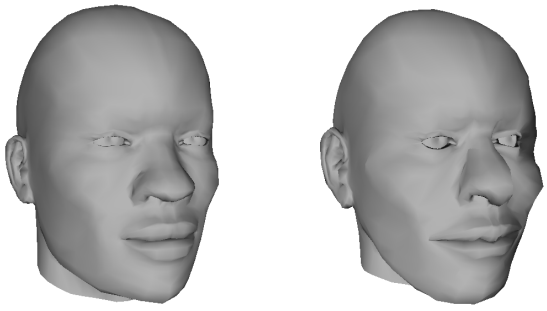

(a) An african negroid male template

(b) Result for the caucasoid male test subject (Fig. 10d)

Fig. 13. Ethnicity limitation

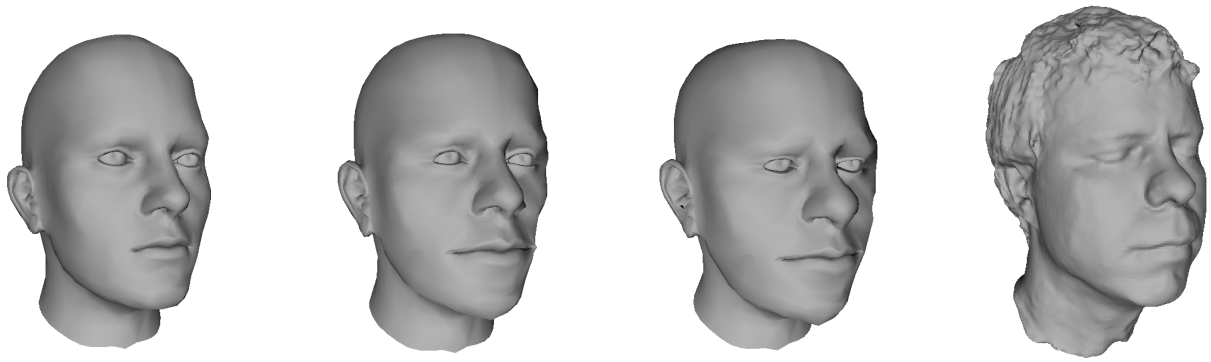

(a) Caucasoid male template

(b) Template deformed with MLS

(c) Template deformed with detail transfer over HRBF

(d) Scanned face of the caucasoid male test subject

Fig. 10. Template, deformations and scanned face comparison for caucasoid male

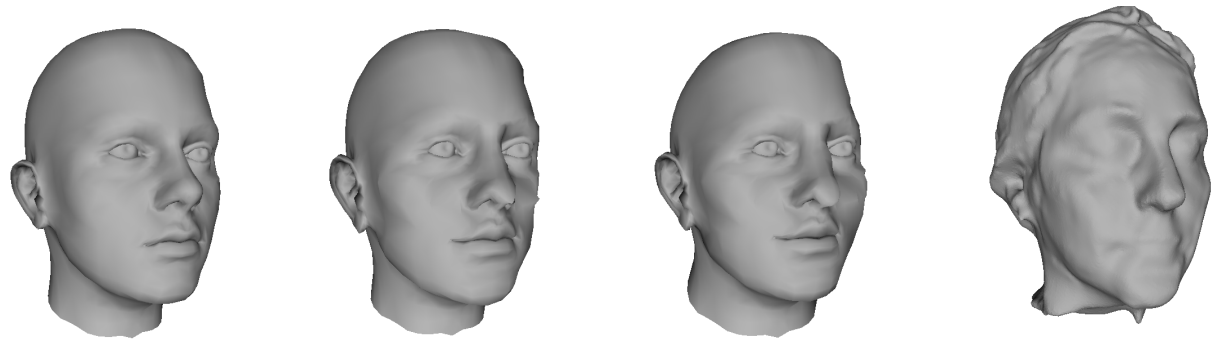

(a) Caucasoid female template

(b) Template deformed with MLS

(c) Template deformed with detail tranfer over HRBF

(d) Scanned face of the caucasoid female test subject

Fig. 11. Template, deformations and scanned face comparison for caucasoid female

VII. Conclusion and future works

In this work a wide series of anatomical rules from the facial reconstruction literature were translated into geometrical restrictions to enhance the anatomical knowledge of the system. Our novel HRBF detail transfer method for facial reconstruction provides a smooth surface while at the same time preserving the topology of the template mesh. The dissociation between detail and overall shape presented by our deformation method significantly reduces the bias towards the template.

Our first informal tests led to successful identification of the subjects. However, broader and more rigorous tests must still be conducted.

The automatic reconstruction only takes a few seconds, being a major advantage over any manual method. However, the manual placement of the craniometric points can be time consuming. Therefore, the creation of guides or computational aids for this part of the process would be a big improvement regarding its usability. In this work we only addressed the geometry of the reconstructed face and thus the visual quality of our result could be enhanced with the use of rendering techniques such as skin, hair and eye shaders. Also, new restrictions could be added to adapt the soft tissue structures of the template to the skull even further.

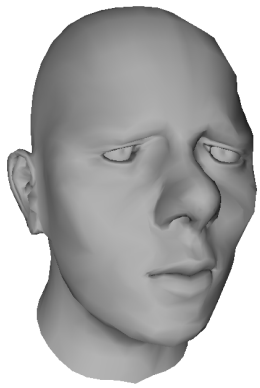

Fig. 14. Caucasoid template (Fig. 10a) deformed for the caucasoid male test subject (Fig. 10d) with detail transfer over HRBF without anatomical rules. It still meets the craniometric constraints perfectly

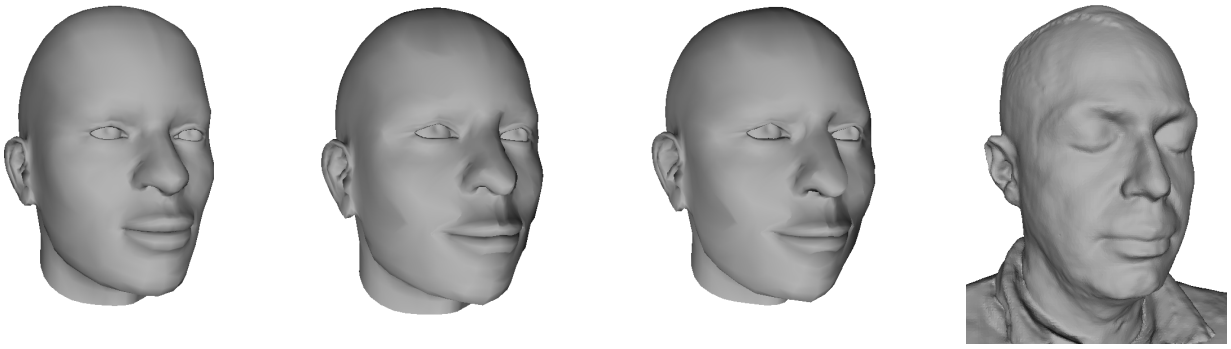

(a) Negroid male template (b) Template deformed with MLS (c) Template deformed with detail tranfer over HRBF (d) Scanned face of the negroid male test subject

Fig. 12. Template, deformations and scanned face comparison for negroid male

ACKNOWLEDGMENT

The first author acknowledges CAPES (Coordenação de Aperfeiçoamento de Pessoal de Nível Superior) for providing his grant. The authors would like to thank Emilio Vital Brazil for his invaluable help with the HRBF library.

REFERENCES

[1] C. Wilkinson, "Facial reconstruction anatomical art or artistic anatomy?" *Journal of Anatomy*, vol. 216, no. 2, pp. 235–250, 2010.

[2] L. Pascual, C. Redondo, B. Sanchez, D. Garrido, and A. Galdon, "Computerized three-dimmensional craniofacial reconstruction from skulls based on landmarks," in *Federated Conference on Computer Science and Information Systems (FedCSIS)*, sept. 2011, pp. 729 –735.

[3] M. Vanezis, "Forensic facial reconstruction using 3-d computer graphics: evaluation and improvement of its reliability in identification," Ph.D. dissertation, University of Glasgow, 2008.

[4] K. Kähler, J. Haber, and H.-P. Seidel, "Reanimating the dead: Reconstruction of expressive faces from skull data," *ACM Trans. Graph.*, vol. 22, no. 3, pp. 554–561, Jul. 2003.

[5] Y. Hu, F. Duan, B. Yin, M. Zhou, Y. Sun, Z. Wu, and G. Geng, "A hierarchical dense deformable model for 3d face reconstruction from skull," *Multimedia Tools and Applications*, vol. 64, no. 2, pp. 345–364, May 2013.

[6] W. Turner, R. Brown, T. Kelliher, P. Tu, M. Taister, and K. Miller, "A novel method of automated skull registration for forensic facial approximation," *Forensic science international*, vol. 154, no. 2, pp. 149–158, November 2005.

[7] F. Duan, S. Yang, D. Huang, Y. Hu, Z. Wu, and M. Zhou, "Craniofacial reconstruction based on multi-linear subspace analysis," *Multimedia Tools and Applications*, pp. 1–15, January 2013.

[8] I. Macedo, J. P. Gois, and L. Velho, "Hermite radial basis functions implicits." *Comput. Graph. Forum*, vol. 30, no. 1, pp. 27–42, 2011.

[9] E. E. Catmull and R. R. J., "A class of local interpolating splines." *Computer Aided Geometric Design*, pp. 317–326, 1974.

[10] A. Cuno, C. Esperança, A. Oliveira, and P. Cavalcanti, "3d as-rigid-as-possible deformations using mls," *In: Proceedings of the 27th Computer Graphics International Conference, Petropolis, RJ, Brazil*, p. 115122, May 2007.

[11] C. Rynn, C. Wilkinson, and H. Peters, "Prediction of nasal morphology from the skull," *Forensic Sci Med Pathol.*

[12] Gerasimov, "The reconstruction of the face on the skull," 1955.

[13] M. Prokopec and D. H. Ubelaker, "Reconstructing the shape of the nose according to the skull," Paper presented at the 9th Biennial Meeting of the International Association for Craniofacial Identification, FBI, Washington, DC, July 2000.

[14] B. E. Hoffman, D. A. McConathy, M. Coward, and L. Saddler, "Relationship between the piriform aperture and interalar nasal widths in adult males," *J. Forensic Sci.*

[15] W. M. Krogman, *The Human Skeleton in Forensic Medicine*. Springfield, IL: Charles C Thomas, 1962.

[16] S. L. Davy-Jow, S. J. Decker, and J. M. Ford, "A simple method of nose tip shape validation for facial approximation," *Forensic Science International*, vol. 214, no. 1, pp. 208.e1–208.e3, January 2012.

[17] C. Stephan and P. Davidson, "The placement of the human eyeball and canthi in craniofacial identification," *J. Forensic Sci.*

[18] C. Stephan, A. Huang, and P. Davidson, "Further evidence on the anatomical placement of the human eyeball for facial approximation and craniofacial superimposition," *J. Forensic Sci.*

[19] J. Kunjur, T. Sabesan, and V. Ilankovan, "Anthropometric analysis of eyebrows and eyelids: An inter-racial study," *British Journal of Oral and Maxillofacial Surgery*, vol. 44, no. 2, pp. 89–93, April 2006.

[20] Y. Choi and S. Eo, "Two-dimensional analysis of palpebral opening in blepharoptosis: visual iris-pupil complex percentage by digital photography," *Annals of plastic surgery*, vol. 72, no. 4, pp. 375–380, April 2014.

[21] K. P. Mashige, "A review of corneal diameter, curvature and thickness values and influencing factors," *The South African Optometrist*, vol. 72, no. 4, pp. 185–194, December 2013.

[22] L. Farkas, M. Katic, T. Hreczko, C. Deutsch, and I. Munro, "Anthropometric proportions in the upper lip-lower lip-chin area of the lower face in young white adults," *American journal of orthodontics*, vol. 86, no. 1, pp. 52–60, July 1984.

[23] G. V. LEBEDINSKAYA, T. S. BALUEVA, and E. V. VESELOVSKAYA, *Forensic Analysis of the Skull*. Wiley-Liss, 1993, ch. 14, p. 183198.

[24] C. Stephan and M. Henneberg, "Predicting mouth width from intercanine width - a 75725–727, July 2003.

[25] C. Wilkinson, M. Motwani, and E. Chiang, "The relationship between the soft tissues and the skeletal detail of the mouth," *Journal of Forensic Sciences*, vol. 48, no. 4, pp. 728–732, July 2003.

[26] W. Wong, D. Davis, M. Camp, and S. Gupta, "The relationship between the soft tissues and the skeletal detail of the mouth," *Journal of plastic, reconstructive & aesthetic surgery*, vol. 63, no. 12, pp. 2032–2039, February 2010.

[27] B. A. FEDOSYUTKIN and J. V. NAINYS, *Forensic Analysis of the Skull*. Wiley-Liss, 1993, ch. 15, p. 199213.

[28] C. Sforza, G. Grandi, M. Binelli, D. G. Tommasi, R. Rosati, and V. F. Ferrario, "Age- and sex-related changes in the normal human ear," *Forensic Science International*, vol. 187, no. 1, pp. 110.e1–110.e7, May 2009.

[29] W. Santos, "Mensuração de tecidos moles da face de brasileiros vivos em imagens multiplanares de ressonância magnética nuclear (rmn) para fins médico-legais," Thesis, Universidade de São Paulo, Ribeirão Preto, 2008.

[30] S. D. Greef, P. Claes, D. Vandermeulen, W. Mollemans, P. Suetens, and G. Willems, "Large-scale in-vivo caucasian facial soft tissue thickness database for craniofacial reconstruction," *Forensic Science International*, vol. 159, no. Supplement, pp. S126–S146, May 2006.